BOND FAILURE INVESTIGATION OF CFRP-STEEL ADHESIVE JOINTS

S. P. Chiew*, S. T. Lie, C. K. Lee and Y. Yu

School of Civil and Environmental Engineering
Nanyang Technological University, Singapore
**(Email: cspchiew@ntu.edu.sg Fax: +65- 6792 1650)*

ABSTRACT: To strengthen deteriorated steel structures, bonding carbon fiber reinforced polymer laminate externally to the steel surface is a promising method. For CFRP-strengthened steel structures, the bond performance between CFRP laminate and steel is a crucial consideration, which will directly influence strengthening effect and determine the final capacity of the strengthened structures. To investigate the bond failure mechanism of CFRP-bonded steel structures, tests for different types of CFRP-steel adhesive joints have to be conducted first. Besides the experimental studies, finite element analyses for the different types of joints are carried out to study in detail the stress and strain distributions along the bondline. It is found that for all joints with different geometries and loading conditions, the most important factors that influence the final bond failure are their peel and in-plane shear stress/strain components. Based on the test results and the finite element analyses, a bond failure model is proposed. With this bond failure model, the failure loads for the different joints can be predicted reasonably well compared to the experimental measurements.

Keywords: Carbon fiber reinforced polymer, adhesive joint and bond failure

1. INTRODUCTION

As an advanced composite material, carbon fiber reinforced polymer (CFRP) has been widely used to strengthen and repair structural concrete elements for years. The desirable characteristics of CFRP such as: high strength, high tensile modulus, light weight, installation facility and resistance to corrosion have all played a very significant role in creating this greater interest for structural repair and strengthening applications. In recent years, it has been found by some researchers that besides strengthening concrete structures, CFRP laminates can also be used to strengthen existing steel structures by external bonding (Miller et al [1], Tavakkolizadeh and Saadatmanesh [2], Jiao and Zhao [3]).

For CFRP-bonded steel structures, a very important concern is the potential bond failure between the CFRP laminate and steel surface. According to the past research results about structural bonded joints (Tong and Steven [4]), the dominant failure mode for composite-bonded metal joint is adhesive failure rather than adherend failure, which is totally different from the “rip-off” failure mode for CFRP-bonded concrete structures. For the later, the strength of the bond between CFRP laminate and concrete surface is generally larger than the failure strength of concrete. Therefore, in the rip-off failure the surface concrete comes off with CFRP. However, for CFRP-bonded steel structures, the failure strengths of steel and CFRP are both very large compared to that of the adhesive bond. Due to material discontinuity at the location of bond end or crack tip, the stress concentration in these areas may cause adhesive failure before steel and CFRP achieve their ultimate strengths. For this reason, the CFRP-steel bond property needs to be studied carefully. In recent years, some researchers have started to focus on this important issue through both experimental and theoretical investigations (Ono et al [5], El Damatty and Abushagur [6]).

Unfortunately, there is still no failure model for CFRP-bonded steel structures which can be used reliably with respect to different geometries and loading conditions.

In this current study, tests for different CFRP-steel adhesive joints are performed. Besides the experimental investigation, the finite element analysis (FEA) is conducted to explore the stress and strain distributions along the bondline. Through analyses of the numerical results of CFRP-steel adhesive joints with different geometries and loading conditions, a bond failure model composed of strain and strain energy components is proposed. The failure loads for the tested joints are well predicted by the proposed bond failure model.

2. EXPERIMENTAL INVESTIGATION

A total of four types of CFRP-steel adhesive joints with different geometries were constructed and tested under monotonic loading to investigate the bond failure behaviours.

2.1 Material Properties

The CFRP laminate used in the experiment is TYFO SCH-41S. This is a commonly used carbon fiber composite material composed of unidirectional carbon fibers with Aramid cross fibers. The adhesive material is TYFO-S saturant epoxy which is a two-component epoxy. The steel type is low carbon S275. The mechanical properties of carbon fiber and laminate are shown in Table 1. The mechanical properties of steel and epoxy are listed in Table 2 and Table 3, respectively.

Table 1. Material Properties of Carbon Fiber and Laminate

Material	Tensile Strength (N/mm^2)	Tensile Modulus (kN/mm^2)	Poisson's Ratio	Elongation (%)	Laminate Thickness (mm)
Carbon Fiber	3790	230.0	0.29	1.7	-
Laminate	876	72.4	0.31	1.2	1

Table 2. Material Properties of Epoxy

Yield Stress (N/mm^2)	Young's Modulus (kN/mm^2)	Elongation Percent	Poisson's Ratio
72.4	3.18	5%	0.35

Table 3. Material Properties of Steel

Yield Stress (N/mm^2)	Young's Modulus (kN/mm^2)	Ultimate Stress (N/mm^2)	Poisson's Ratio
280	200	420	0.3

2.2 Test Specimen

To obtain the bond strength of joints under different loading conditions, the following specimens are designed as: (a) Double-lap joint, (b) Single-lap joint, (c) T-peel joint and (d) Tubular joint. The configurations of the four types of joint specimens are illustrated in Figure 1. To investigate the bond strength under shear dominant loading case, double-lap joint specimens are employed as well as tubular joints. T-peel and single-lap joint specimens are respectively employed to investigate peel and mixed loading effects, respectively. The dimensions of the specimens mentioned above are

shown in Table 4. The four types of joints are abbreviated to: DL (double-lap), SL (single-lap), TP (T-peel) and TB (tubular). For each type of joints, Arabic numerals are used to indicate the sub-types (joints with same configurations but different dimensions). The thickness of adhesive layer is around a constant value of 0.15mm for all the joints.

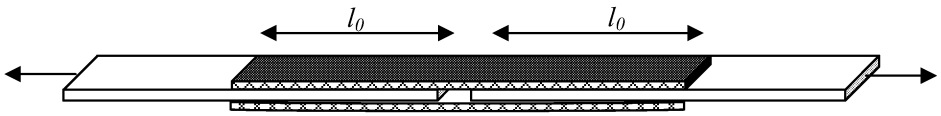

(a) Double-lap joint

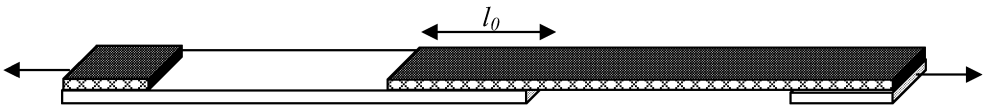

(b) Single-lap joint

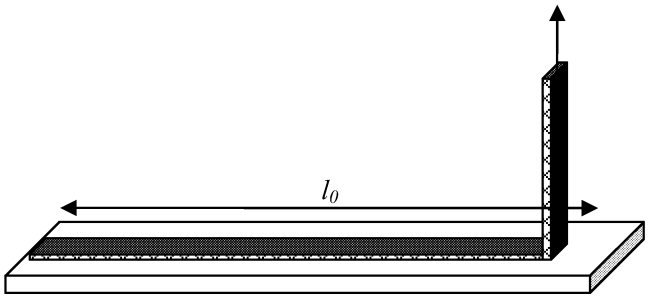

(c) T-peel joint

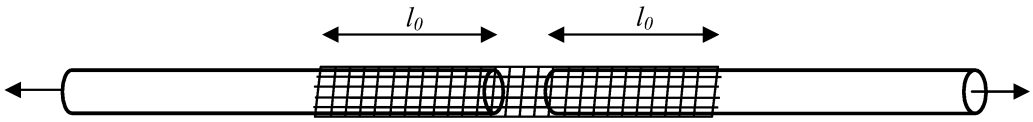

(d) Tubular joint

Figure 1. Joint specimen configurations

Table 4. Specimen Dimensions and Average Failure Loads of Bond Tests

Specimen Type	Number of Specimens	Thickness of Steel Adherend (mm)	Bond Length (mm)	Bond Width (mm)	Average Failure Load (kN)
DL1	3	2.0	12.7	25.4	3.9
DL2	1	2.0	50.8	50.8	22.5
DL3	1	2.0	100.0	50.8	27.5
DL4	1	2.0	150.0	50.8	27.8
DL5	1	2.0	200.0	50.8	25.8
SL1	3	2.0	25.4	25.4	3.1
SL2	1	2.0	50.8	50.8	4.2
TP1	3	6.0	100.0	25.4	0.2
TP2	3	6.0	100.0	50.8	0.4
TB1	3	2.2	200.0	188.4	77.4
TB2	2	2.2	400.0	188.4	92.6

2.3 Specimen Preparation

To guarantee the bond quality, the steel plates are manually grinded with sand paper and the steel tubes are treated with sand blast. This process is to make the steel surface free of protrusions or cavities, which may cause voids in the bondline. Before bonding the CFRP laminates, steel surfaces are cleaned with acetone. The epoxy is mixed of 100 parts of component A and 42 parts of component B by volume. While the CFRP laminates being bonded, they are carefully pressed with special rollers to ensure that there is no air hump remained. After the laminates are adhered, no extra pressure is exerted during curing. The extra epoxy are cut off carefully and removed from the specimens after a curing period of 72 hours. For tubular specimens, a steel solid bar is welded on each end of the tube for clamping purpose.

For each double and single plate joint, two strain gauges are placed on the steel and CFRP adherend respectively to monitor the strain increment in the loading process. For the 200mm tubular joint, nine strain gauges are placed on the CFRP adherend to investigate the strain variation along the axial direction. The positions of the strain gauges are illustrated in Figure 2.

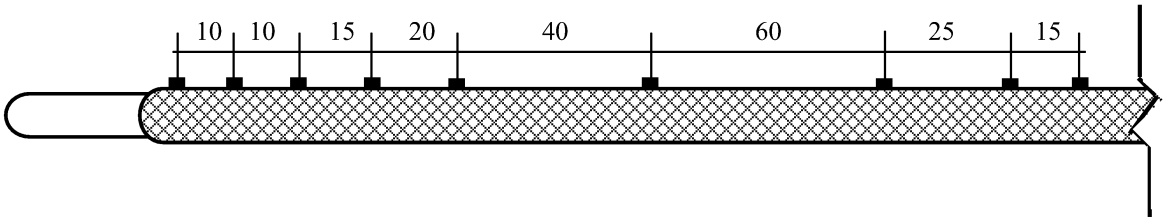

Figure 2. Illustration of the positions of strain gauges on CFRP laminate (unit: mm)

2.4 Test Procedure and Results

Two types of universal testing machines are used as loading equipment. For double-lap, single-lap and T-peel joints, the Instron 5500 universal electro-mechanical testing system is used. The loading speed for these specimens is 0.01mm/s. For tubular joints, the Instron 5590 universal hydraulic testing system is employed to satisfy the requirement of larger dimensions and higher forces. A loading speed of 0.02mm/s is employed. As expected, the failure mode of all the specimens is adhesive bond failure. The CFRP and steel adherends separate under failure load without damage in

the CFRP laminate. The pictures of intact and damaged typical specimens are shown in Figure 3. The average failure load of each type of specimen is listed in Table 4.

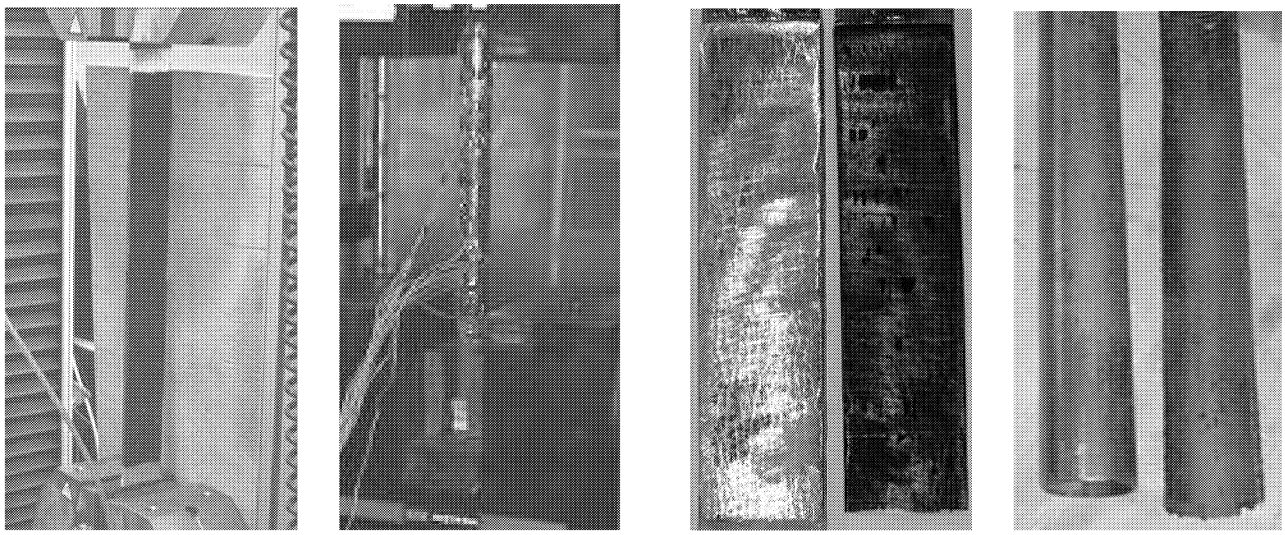

(a) Before failure (b) After failure

Figure 3. Typical specimens before and after failure

For the joints under in-plane loading, i.e. double-lap and tubular joints, the bond strengths are not proportional to the bond lengths. For double-lap joint specimens, the strength in unit length is defined as,

$$S = P/(2b) \tag{1}$$

where P is the ultimate load for the specimen and b is the plate width. For tubular joints, the strength in unit length is defined as following,

$$S = P/(2\pi R) \tag{2}$$

The bond strength varying trend is shown in Figure 4. The longer the bond length is, the more slowly the bond strength increases. When the bond length is large enough, the strength increase with the rising length tends to be unnoticeable. This phenomenon is quite similar with what exists in the adhesively bonded metal joints (Sheppard et al [7]).

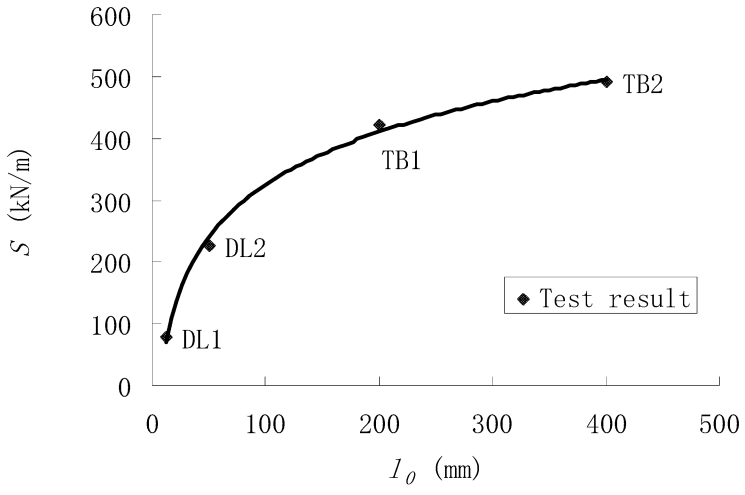

Figure 4. Relationship between bond strength and bond length

In Figure 5 the strain distribution in the CFRP laminate is shown. L is the distance from the end of the laminate. It can be seen in the major part of the CFRP laminate the strain distributes evenly, while at the CFRP and steel ends the strain varies sharply, especially at the later one. Because the cross-section magnitude of stiffness of the internal steel tube is larger than that of the CFRP laminate, more loads is shared by steel than CFRP in the middle region where CFRP and steel bear together. At the end of the steel tube, load transferred into CFRP laminate is much more than that at the CFRP end, so the stress/strain in the CFRP laminate increases even faster.

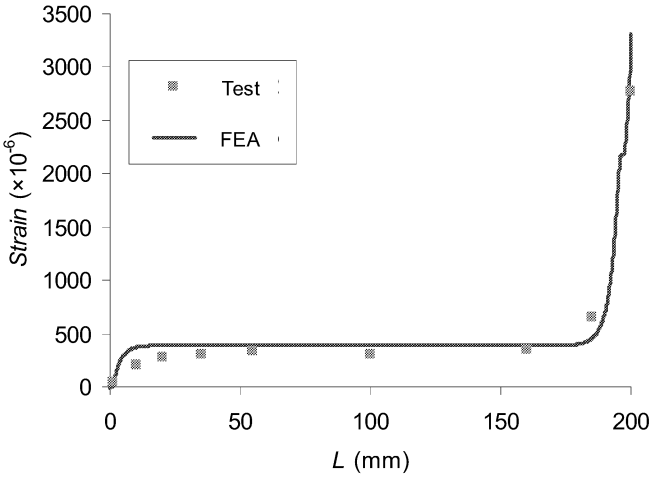

Figure 5. Strain distribution along the CFRP laminate for TB1

3. NUMERICAL ANALYSIS

3.1 Finite Element Modelling Technique

To analyze the adhesively bonded joints tested above, the FE software package ABAQUS (Version 6.4-1) is used in this study. Isoparametric, three-node and four-node plane strain elements are employed to model the joints. Material nonlinearity is also incorporated in the analysis to simulate the constitutive relationship of the adhesive and the steel adherend. The Von Mises yield criterion is used for both adhesive layer and steel adherend.

Both the adherends and the adhesive are modelled as separate parts and linked together. A pairs of nodes at each identical location exists at the material interfaces, one belonging to the adherend, the other to the adhesive. All degrees of freedom of the corresponding nodes are constrained to identical displacements. This approach is necessary to obtain accurate stress and failure ratio results at the interface, i.e. to obtain stress jumps at the interface due to the stiffness jumps between the different materials. Also, it is important to take the geometric nonlinearity into account. The relative displacement between CFRP and steel adherend changes the stress distributions in adherends and adhesive under loading. Hence, the stress distributions under at small loads often differ considerably from the distributions at high loads.

In the FE analysis of FPR-steel joints, what are of most concern are the stress and strain distributions in the adhesive layer, because the failure mode of the joints is adhesive failure. The adhesive layer is very thin compared with the thickness of the adherends but, to achieve reliable results, it is necessary to use fine mesh for the adhesive and the regions in the adherends close to the adhesive. Other further regions, such as the adherends outside the joint overlap, can be

modelled with a coarser mesh. On the other hand, too fine mesh may lead to rather high number of degrees of freedom, which is time-consuming and it further complicates the pre- and post-processing of the analysis. With reference to Sheppard et al. [7], the adhesive layer should be meshed in the dimension of adhesive thickness, and the consequent FE analysis results would be quite good. Accordingly, one layer of elements is used for the adhesive; and four to seven layers of elements are employed for the adherends.

3.2 Stress/Strain Distribution

In CFRP-retrofitted structures, the most significant role the adhesive play is stress transition. Generally, when the original structure is retrofitted by CFRP, the external loads do not exert on the laminates directly. The load in the longitudinal direction in CFRP comes from the original structure by the stress transfer through the adhesive layer. In this process the adhesive layer undergoes a large shearing deformation. Therefore, the shearing stress and strain distributions in adhesive should be given much attention. Hart-Smith [8] discussed that only for very short overlap test coupons is the strength a function of the bond area. For long overlap bonded joints the strength is uniform, with the great majority of the load carried by the plastic adhesive zones separated by the lightly loaded elastic trough. The width of these plastic zones is constant regardless of the overlap. However, if one of the adherends had been less stiff than the other, the load transfer would not have been balanced and the adhesive could be critically strained at one end (from which the softer adherend extended) before a significant load transfer had developed at the other end.

To illustrate the point discussed above, the shearing stress in the adhesive layer and the tension stress in the midline of steel and CFRP are plotted in Figure 6. In the graph, x is the normalized distance from the end of the CFRP laminate. It can be seen that from left to right, the stress in steel drops from maximum value to zero. To keep the section load balanced, the stress in CFRP increases so that the load transfers gradually from steel to CFRP laminate. The major part of load transfer happens in the area near the joint ends, while in the middle section of the joint the stresses are stably distributed according to the stiffness of steel and CFRP. Therefore, the value of shearing stress in the adhesive end is very large as a result of stress transfer between steel and CFRP. In the middle section where the stresses in steel and CFRP are more stable, the shearing stress in adhesive is close to zero.

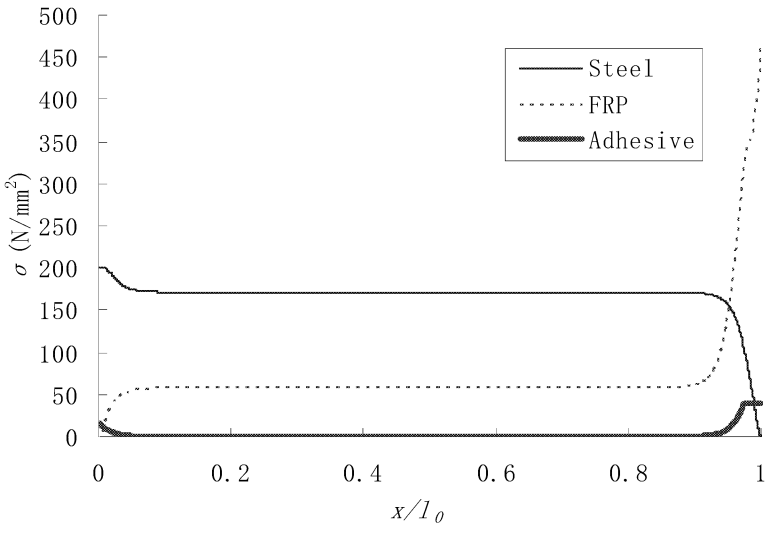

Figure 6. Stress distributions in adherends and adhesive for TB1

Based on the FE analysis of double-lap and tubular joints with different bond lengths, the shearing stress distributions in the adhesive layers are shown in Figure 7. It can be seen that for the joint with relatively short bond length, the maximum stress in the joint end does not reach the maximum shearing stress of the adhesive at the moment the joint fails, and the stress in the middle section of the joint is of high value. With increasing bond length, the stress in the joint end goes up. For the joint with 200mm bond length, the maximum shearing stress has been attained in the joint end before the joint fails. The stress in the middle section keeps relatively low value till the joint fails. This is similar to the stress distribution of conventional symmetric double-lap metal joints. Compared to the conventional symmetric double-lap metal joints, an essential difference of the CFRP-steel joint is that the stress values are not equal in each end of the joint. It is shown that the stress value at the left end of the joint is two more times less than that at the right. This phenomenon is caused by the stiffness difference between the upper and lower adherends. Since the CFRP laminate is less stiff than steel, the stress at the joint end where the steel adherend terminates is much higher than the stress at the other end. Therefore, the bond failure initiates from the end where the steel adherend terminates. This conclusion agrees with the test observation.

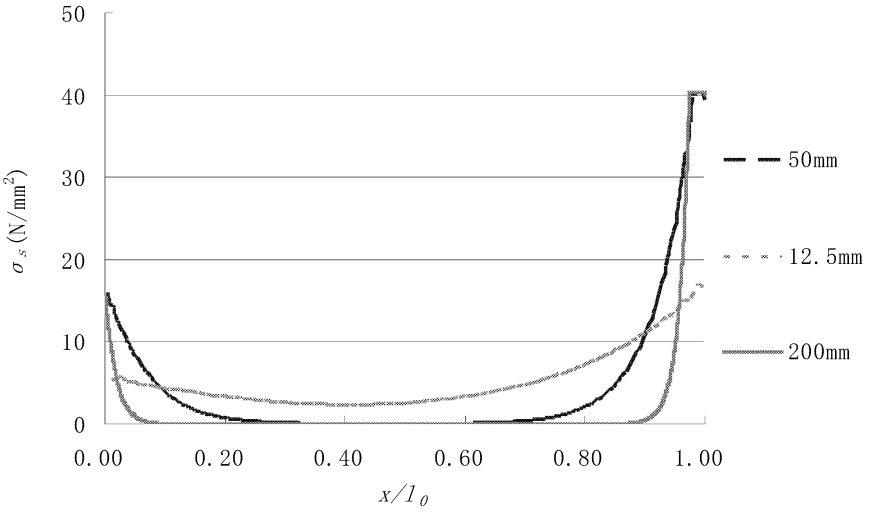

Figure 7. Comparison of stress distributions along the bondlines

In the adhesive layer, the normal stress and strain at the joint ends are not negligible. Generally the magnitude of peel stress and strain is much less than that of relevant shearing components for in-plane loaded joints. However, for adhesive materials, the volume deformation capacity is not as good as shape deformation capacity, which means the normal strain to cause the adhesive failure could be much smaller compared to the shearing strain.

Generally, the failure of adhesive joints always initiate from the joint end no matter what the joint geometry is. By FE analysis of different joints, the typical shearing and normal strain distributions in the double-lap, single-lap and T-peel joints are illustrated in Figures 8 to 10. It is clear that both shearing and normal strains in the adhesive layer have prominent high values at the joint ends. Also, it can be seen that the adhesive failure of all the joints is the result of the synergetic effect of shearing and normal stresses.

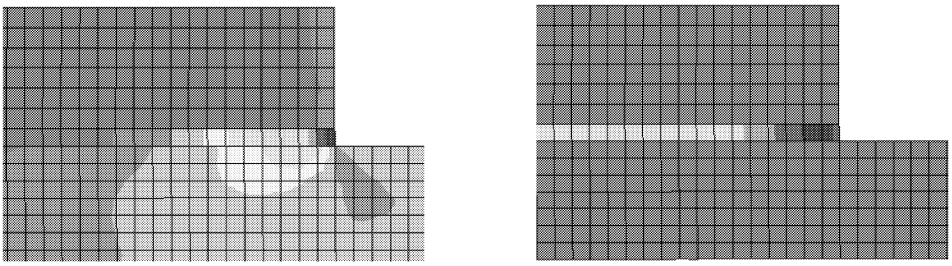

(a) Normal strain (b) Shear strain

Figure 8. Normal and shear strain at the end of typical double-lap or tubular joint

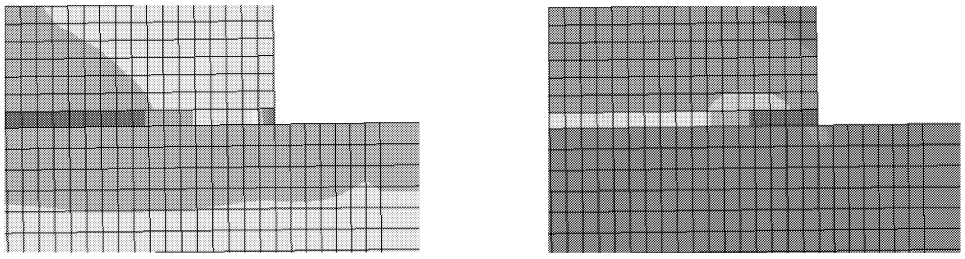

(a) Normal strain (b) Shear strain

Figure 9. Normal and shear strain at the end of single-lap joint

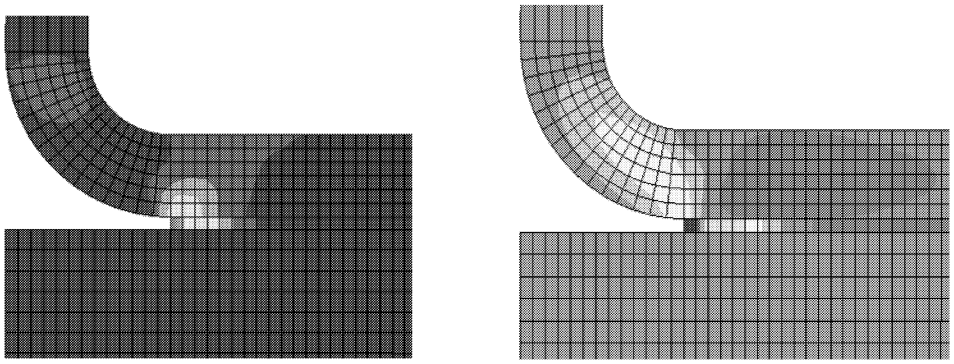

(a) Normal strain (b) Shear strain

Figure 10. Normal strain and shear strain at the end of peel joint

4. BOND FAILURE MODEL

4.1 Stress Investigation

The possibility of employing stress components as failure criterion is studied first. Based on the stress analysis of all the tested joints, different stress components such as shear, normal, deviatoric and hydrostatic stress have been analyzed. In Figure 11, the deviatoric and hydrostatic stress components for the joints are plotted. It is found that, for the joints with different bond lengths or geometries, the adhesives at the joint ends may have very close stress values, while the strains are quite different. This is mainly because the epoxy used in this study is a not an elastic material. Therefore, the stress components are not sensitive enough to be used as the failure indices.

Further more, it was observed by Lee and Kong [9] that the maximum principle stress zone

criterion proposed by Clark and McGregor [10] was not satisfied in the case of adhesively bonded joints composed of dissimilar adherend materials. Due to these reasons, the stress components are not suitable for failure criterion construction.

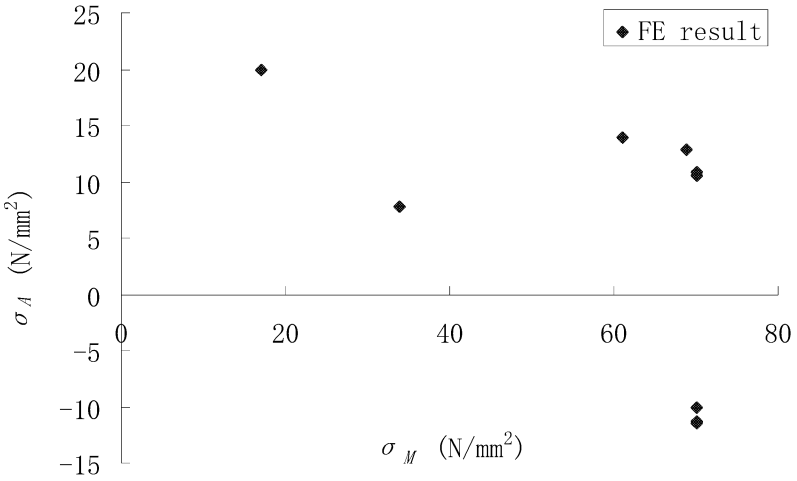

Figure 11. Relationship between deviatoric and hydrostatic stress components

4.2 Strain Investigation

As far as strain components are studied, in-plane shear and normal strain tensors are of most concern since they play a dominant role in adhesive failure mechanism. Based on the experimental and numerical results, the relationship between normal strain and shear strain at failure load of each type of specimen can be obtained. In the region where normal strain is negative, there tends to be a linear relationship between these components as shown in Figure 12.

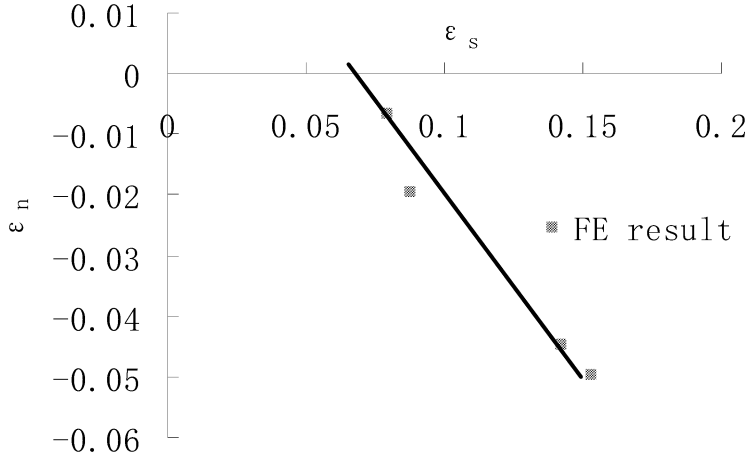

Figure 12. Linear relationship between negative normal and shear strain

This linear tendency is quite similar to the conclusion of Oh et al [11]. In their study, in the region where normal stress is negative, a linear relationship of normal and shearing components is proposed based on the experimental result. Consequently, it is reasonable to employ a linear equation with respect to normal strain and shear strains as the failure criterion in the region with negative normal strain. Therefore, the adhesive failure model in the region with negative normal strain can be proposed as,

$$\frac{\varepsilon_s}{\varepsilon_{sc}} + \frac{\varepsilon_n}{\varepsilon_{nc}} = 1 \tag{3}$$

where ε_n is normal strain, ε_s is shear strain, and ε_{sc} and ε_{nc} are the critical value of shear and normal strain, respectively. From Figure 5, their values are derived as 0.07 and 0.05.

4.3 Strain Energy Density Investigation

For the specimens in which the peel components play a relatively dominant role in the adhesive failure process, the linear equation of normal and shearing strain is not suitable any more. According to Tong and Steven [4], the mixed-mode failure criterion for solid fracture can be expressed in a linear equation with respect to energy release rates, which is a quadratic variable with respect to stress or strain. Therefore, in this study, a quadratic variable about strain is then taken into consideration, which is strain energy density. The general expression of strain energy density is,

$$w = \int_0^{\varepsilon_{ij}} \sigma_{ij} d\varepsilon_{ij} \tag{4}$$

where σ_{ij} and ε_{ij} are stress and strain tensors, respectively. In this study, the relationship between shear strain energy and peel strain energy of the peel strain involved specimens is shown in Figure 13.

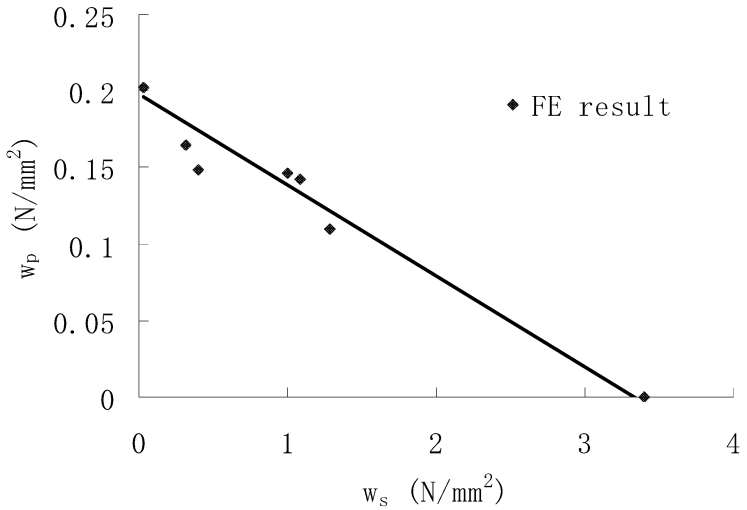

Figure 13. Linear relationship between peel and shear strain energy density

It is clear that the relationship of these two variables can be approximately formulated by a linear equation. So, when the normal strain is positive, the adhesive failure model is proposed as

$$\frac{w_s}{w_{sc}} + \frac{w_p}{w_{pc}} = 1 \tag{5}$$

where w_{sc} is the critical shear energy density, and w_{pc} is the critical peel energy density. The shear strain energy density is defined as

$$w_s = \int_0^{\varepsilon_s} \sigma_s d\varepsilon_s \tag{6}$$

where σ_s is shear stress. Similarly, the peel strain energy is defined as follow:

$$w_p = \int_0^{\varepsilon_p} \sigma_p d\varepsilon_p \tag{7}$$

where σ_p is peel stress, and ε_p is peel strain. The value of the critical shear strain energy density is deduced as 3.55 and for peel strain energy density that value is 0.2.

4.4 Failure Prediction for CFRP-Steel Joints

With the adhesive failure criterion proposed above, the failure loads of the tested specimens are predicted by the FE analysis. Failure is to occur in each joint when the adhesive shearing and normal strain index reaches the critical value or when the strain energy density criterion is satisfied. Table 5 shows the failure load comparison of experimental and numerical results for each type of the CFRP-steel adhesive joints. It is argued that due to the wide range of bonded joint types, the accuracy of the failure predictions is reasonably good.

Table 5. Comparison of Experimental and Numerical Bond Strengths

Model	Failure Load from Test P_{av} (kN)	Failure Load from FEA P_n (kN)	Load Difference ΔP (kN)	Comparative Load Difference $\lvert\Delta P\rvert / P_{av}$
DL1	3.9	3.9	0.0	0.00
DL2	22.5	25.3	2.8	0.12
DL3	27.5	27.5	0	0.00
DL4	27.8	27.5	-0.3	0.01
DL5	25.8	27.5	1.7	0.07
SL1	3.1	3.5	0.4	0.13
SL2	4.2	5.1	0.9	0.21
TP1	0.2	0.2	0.0	0.00
TP2	0.4	0.4	0.0	0.00
TB1	77.4	78.4	1.0	0.01
TB2	92.6	85.8	-6.8	0.07

5. CONCLUSION AND FUTURE WORK

For CFRP-steel adhesive joints, debonding failure is a very important consideration. Bond failure between CFRP laminate and steel surface is the only failure mode for the four types of joints discussed in this paper. For joint with bondline parallel to the loading direction, the bond failure load increases with the bond length. The longer the bond length, the smaller is this increment. When the bond length reaches a certain value, the strength increment tends to be insignificant with correspondingly increasing bond length. As a result of the high stress/strain concentration, debonding failure for all joints initiates from the end of bondline.

A bond failure model composed of strain and strain energy criteria is proposed for the CFRP-steel adhesively bonded joints. When this bond failure model is incorporated in the numerical analysis, the bond failure loads for the different CFRP-steel adhesive joints can be predicted. The numerical prediction for the bond failure loads agree reasonably well with the experimental measurements.

REFERENCES

[1] Miller T.C., Chajes M.J., Mertz D.R. and Hastings J.N., "Strengthening of a steel bridge girder using CFRP plates", Journal of Bridge Engineering, ASCE, 2001, 6(6), pp. 514-522.

[2] Tavakkolizadeh M. and Saadatmanesh H., "Fatigue strength of steel girders strengthened with carbon fiber reinforced polymer patch", Journal of Structural Engineering, ASCE, 2003, 129(2), pp. 186–196.

[3] Jiao, H. and Zhao, X. L., "CFRP strengthened butt-welded very high strength (VHS) circular steel tubes", Thin-Walled Structures, 2004, 42(7), pp. 963-978.

[4] Tong L. and Steven G.P., "Analysis and Design of Structural Bonded Joints", Kluwer Academic, Boston, USA, 1999.

[5] Ono K., Sugiura K., Sasaki A., Wakahara N. and Komaki H., "Bond characteristics of carbon fiber reinforced plastics to structural steels", High Performance Materials in Bridges: Proceedings of the International Conference, Kona, Hawaii, 2001, pp. 34-43.

[6] El Damatty A.A. and Abushagur M., "Testing and modeling of shear and peel behavior for bonded steel/CFRP connections", Thin-Walled Structures, 2003, 41(11), pp. 987–1003.

[7] Sheppard A., Kelly D. and Tong L., "A damage zone model for the failure analysis of adhesively bonded joints", International Journal of Adhesion & Adhesives, 1998, 18(6), pp. 385–400.

[8] Hart-Smith, L. J., "Adhesive bond of aircraft primary structures", High-Performance Adhesive Bond, Dearborn, Michigan, USA, 1980, pp. 1-17.

[9] Lee, K.Y. and Kong, B.S., "Theoretical and experimental studies for the failure criterion of adhesively bonded joints", Journal of Adhesion Science and Technology, 2000, 14(6), pp. 817-832.

[10] Clarke J.D. and McGregor I.J., "Ultimate tensile stress over a zone: a new failure criterion for adhesive joints", Journal of Adhesion, 1993, 42(3), pp. 227-245.

[11] Oh, B. H., Cho, J. Y. and Park, D. G., "Failure behaviour and separation criterion for strengthened concrete members with steel plates", Journal of Structural Engineering, ASCE, 2003, 129(9), pp. 1191-1198.

Notations

b	=	Width of adherend
L	=	Distance from the end of laminate
l_0	=	Bond length
P	=	Ultimate load from test
P_n	=	Ultimate load from FEA
ΔP	=	Difference between ultimate loads from test and FEA (P_n-P)
R	=	Outer radius of steel tube
S	=	Bond strength in unit length
w	=	Strain energy density
w_p	=	Peel strain energy density
w_{pc}	=	Critical peel strain energy density
w_s	=	Shear strain energy density
w_{sc}	=	Critical shear strain energy density
x	=	Normalized distance from the end of laminate
π	=	Circular constant
ε_{ij}	=	Strain tensor
ε_n	=	Normal strain
ε_{nc}	=	Critical normal strain
ε_p	=	Peel strain
ε_s	=	Shear Strain
ε_{sc}	=	Critical shear strain
σ	=	Stress
σ_A	=	Hydrostatic stress
σ_{ij}	=	Stress tensor
σ_M	=	Deviatoric stress
σ_p	=	Peel stress
σ_s	=	Shear stress